In Vivo Biological Evaluation of a Synthetic Royleanone Derivative as a Promising Fast-acting Trypanocidal Agent by Inducing Mitochondrial-dependent Necrosis

Rubén Martín-Escolano, Juan J. Guardia, Javier Martín-Escolano, Nuria Cirauqui, Antonio Fernández, Maria J. Rosales, Rachid Chahboun, Manuel Sánchez-Moreno, Enrique Alvarez-Manzaneda,* and Clotilde Marín*

ABSTRACT: The life-long and life-threatening Chagas disease is one of the most neglected tropical diseases caused by the protozoan parasite *Trypanosoma cruzi*. It is a major public health problem in Latin America since six to seven million people are infected, being the principal cause of mortality in many endemic regions. Moreover, Chagas disease has become widespread due to migrant population. Additionally, there are no vaccines nor effective treatments to fight the disease because of its long-term nature and complex pathology. Therefore, these emphasize how crucial the international effort to the development of new treatments against Chagas disease. Here, we present the in vitro and in vivo trypanocidal activity of some oxygenated abietane diterpenoids and related compounds. The 1,4-benzoquinone **15**, not yet reported, was identified as a fast-acting trypanocidal drug with efficacy against different strains in vitro, and higher activity and lower toxicity than benznidazole in both phases of murine Chagas disease. The mode of action was also evaluated, suggesting that quinone **15** kills *Trypanosoma cruzi* by inducing mitochondrion-dependent necrosis through a bioenergetics collapse caused by a mitochondrial membrane depolarisation and iron-containing superoxide dismutase inhibition. Therefore, the abietane 1,4-benzoquinone **15** can be considered as a new candidate molecule for the development of an appropriate and commercially accessible anti-Chagas drug.

Chagas disease (CD), also known as American trypanosomiasis, is caused by tropical infection with the insect-transmitted protozoan parasite *Trypanosoma cruzi*. CD is an important public health problem in Latin America since it is a life-long and life-threatening infection, and the major cause of morbidity and mortality in many endemic regions. A total of six to seven million people are infected and the disease causes about 14,000 deaths annually.[1–4] Hematophagus triatomines (vectors) are the principal route of transmission, although the congenital route, transmission route from donors to transplant or transfusion recipients, and oral route involving parasite-contaminated food and drink are also important.[5–7] Recently, CD has also become more widespread as a result of infected migrant populations, particularly in the United States and Europe.[8–11]

T. cruzi infection is far from innocuous and, in mammal hosts, it is an obligate intracellular parasite for its replication, which can infect most nucleated cells.[12,13] During the initial acute stage of the disease, which occurs 2-8 weeks post-infection in humans, parasites become widely disseminated in tissues and organs and can be detected in the bloodstream, and CD generally manifests as a mild febrile illness. Following suppression of the acute stage by the adaptive immune response,[14,15] the disease progresses to a long-lasting asymptomatic chronic stage, which is characterized by an extremely low parasite burden. However, ~30% of those infected will advance to a symptomatic stage, developing pathology such as cardiomyopathy and digestive tract megasyndromes, outcomes for which there are few therapeutic options.[16–18]

Because of the long-term nature of CD and its complex pathology, there are no vaccines nor realistic prospects of them in the near future. The nitroheterocyclic drugs benznidazole (BZN) and nifurtimox (NFX) are the front-line chemotherapy and have been used to treat *T. cruzi* infections for more than 50 years, although treatment failures are frequently reported, in addition to a range of toxic side-effects and extended

treatment length (60 to 90 days).[19–23] Furthermore, the well-known cross-resistance[24,25] and the natural variation in susceptibility to drugs due to the extreme diversity of species[25,26] exemplify the importance of the international effort aimed at developing new drugs against CD.

Taking into account the urgent need for new drugs with improved efficacy, tolerability and safety, we undertook a study of the trypanocidal activity of some terpenoids (Figure 1). Continuing the research on the activity of phenolic abietane diterpenoids,[27] we focused on investigating the trypanocidal activity of quinones with an abietane skeleton, related to royleanone (**1**). Royleanones are a family of abietane diterpenoids bearing a hydroxy-*p*-quinone C ring, which exhibited a wide variety of biological properties, including antiparasitic. For example, the 6,7-dehydroderivative **2** showed antitermitic[28] and antiprotozoal activity.[29] Derivatives **3** and **4** exhibited antitumor activity, with high selectivity.[30] The 12-deoxyderivative **5** has antileishmanial activity.[31] Structurally related to royleanone are taxodione (**7**), with antileishmanial[32] and cytotoxic activity,[33] and the *nor*-abietane antifungals, taxodal (**8**)[34] and cupressol (**9**).[35]

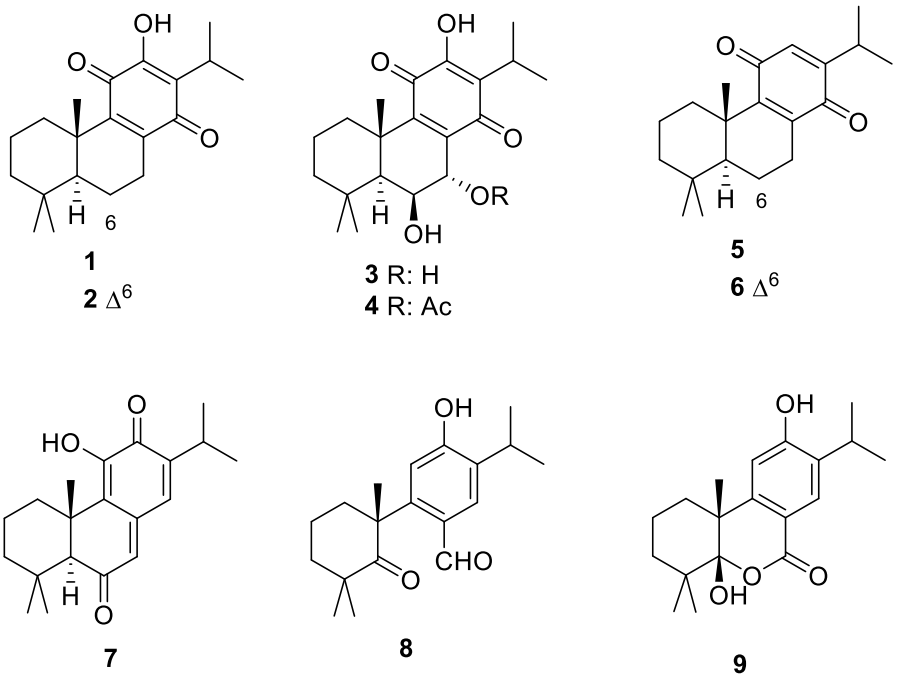

Figure 1. Royleanones and other oxidized abietane and *nor*-abietane diterpenoids.

This paper describes the syntheses of some oxidized terpenoids, phenols, and quinones, with an abietane or *nor*-abietane skeleton and their in vitro and in vivo trypanocidal activity against three different *T. cruzi* strains. The quinone **15**, first reported here, met the majority of the in vitro and in vivo requirements established for ideal drugs against CD, and according to the results we suggest that it exhibits a promising ADMET profile (absorption, distribution, metabolism, excretion and toxicity). Acquiring quinone **15** via a six-step sequence (30% overall yield) from inexpensive abietic acid (**10**), could make it commercially attractive. Therefore, quinone **15** may represent a molecule with potential to be developed into new anti-Chagas drugs. Regarding the mode of action (MoA), we suggest that quinone **15** is a fast-acting trypanocidal drug that induces necrosis in a mitochondrion-dependent manner through a bioenergetic collapse caused by a mitochondrial membrane depolarisation and iron-containing superoxide dismutase (Fe-SOD) inhibition.

RESULTS AND DISCUSSION

Chemistry. The synthesis of terpenoids related to royleanones utilizes abietic acid (**10**), a commercially available and inexpensive diterpenoid, as a starting material. At first glance, the 11,14-dioxygenated function of royleanones cannot be directly achieved, via electrophilic substitution of dehydroabietic acid (**11**), readily obtainable from acid **10**, because the electrophilic attack takes place predominantly at C-12.[36] To circumvent this, 14-hydroxydehydroabietic acid derivatives, such as phenol **13**, were synthesized via regioselective dihydroxylation of abietic acid (**10**)[36] (Scheme 1). Compound **13** was subsequently transformed into phenol **14** and the new quinone **15**. The latter, bearing a 1,4-benzoquinone moiety , is structurally related to royleanones.

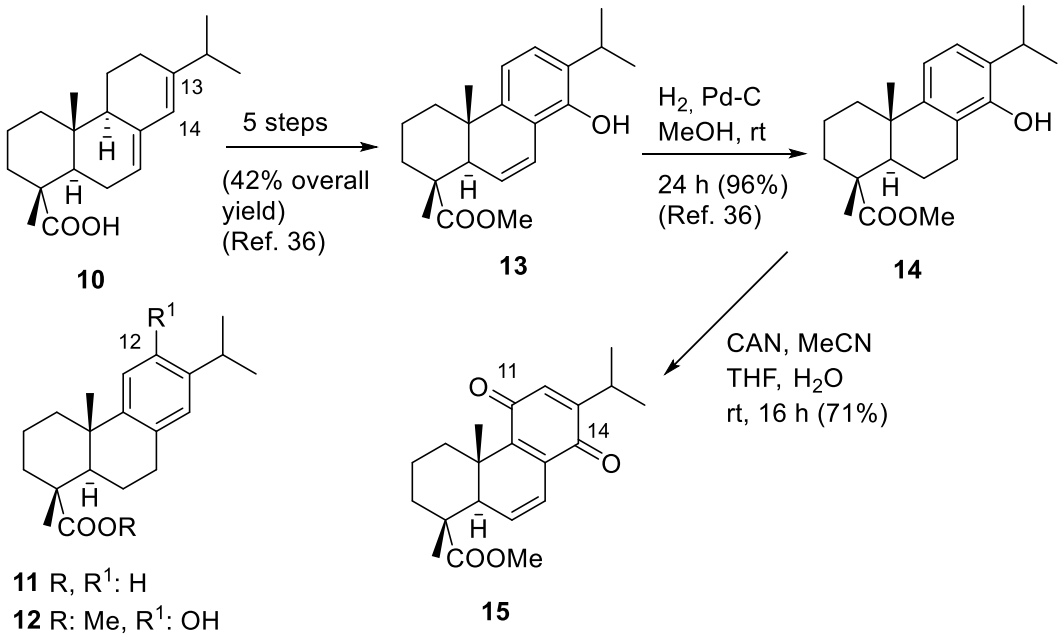

Scheme 1. Synthesis of Phenol **14** and Quinone **15** from Abietic acid (**10**).

Taking into account that the 12-substituted dehydroabietane derivatives, such as phenol **12**, are readily accessible by electrophilic substitution, a protocol for the conversion of these types of compounds into the corresponding 11,14-derivatives, based on B-ring opening and the subsequent B-ring reconstruction was developed (Scheme 2). In this way, sugiol (**16**), a natural terpenoid widely distributed in nature,[37–40] was

transformed into the 11,14-quinone **20**, structurally related to royleanones. The treatment of compound **16** with TFAA in the presence of H_2O_2 gave lactone **17**,[41] which after successive reduction and oxidation afforded the cytotoxic[42,43] quinone alcohol **18** or the quinone aldehyde **19**, depending upon the reaction conditions. The latter underwent fast cyclization, by refluxing with PTSA in benzene, yielding quinone **20.**[44]

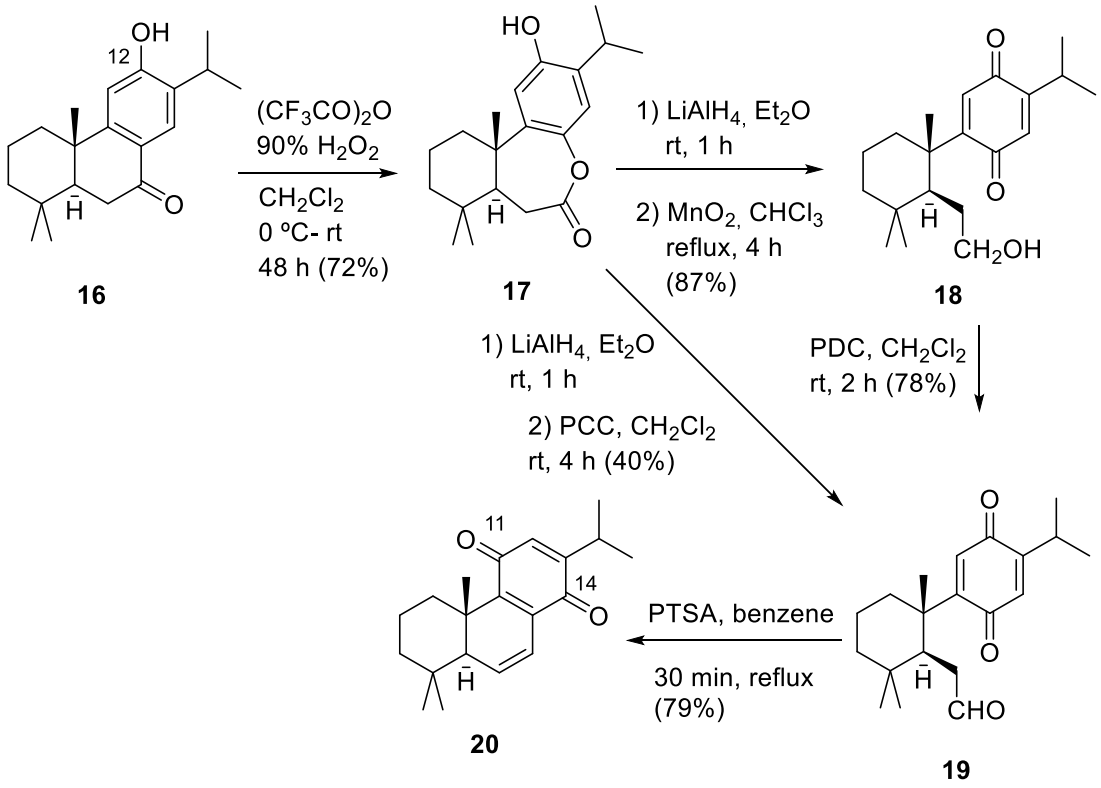

Scheme 2. Synthesis of Quinone **20** from Sugiol (**16**).

Next, the preparation of a taxodione related compound starting from the 12-hydroxy ester **12** was investigated (Scheme 3). Treatment with seleninic anhydride gave the *o*-quinone **21**. Very recently, a four-step sequence (47% overall yield), for the transformation of phenol **12** into quinone **21** has been reported.[45] Interestingly, *o*-quinone **21**, after refluxing with DDQ in dioxane, underwent oxidation at C-6 and the simultaneous 1,2-shift of the angular methyl, leading to the rearranged lactone **22**, structurally related to taxodione (**7**). The natural 18-oxoferruginol (**24**)[46] was also readily prepared from ester **12** after catalytic hydrogenation of the *O*-benzylated **23**,

previously synthesized in our laboratory.[47] The observed and reported spectroscopic data of aldehyde **24** are identical.[48]

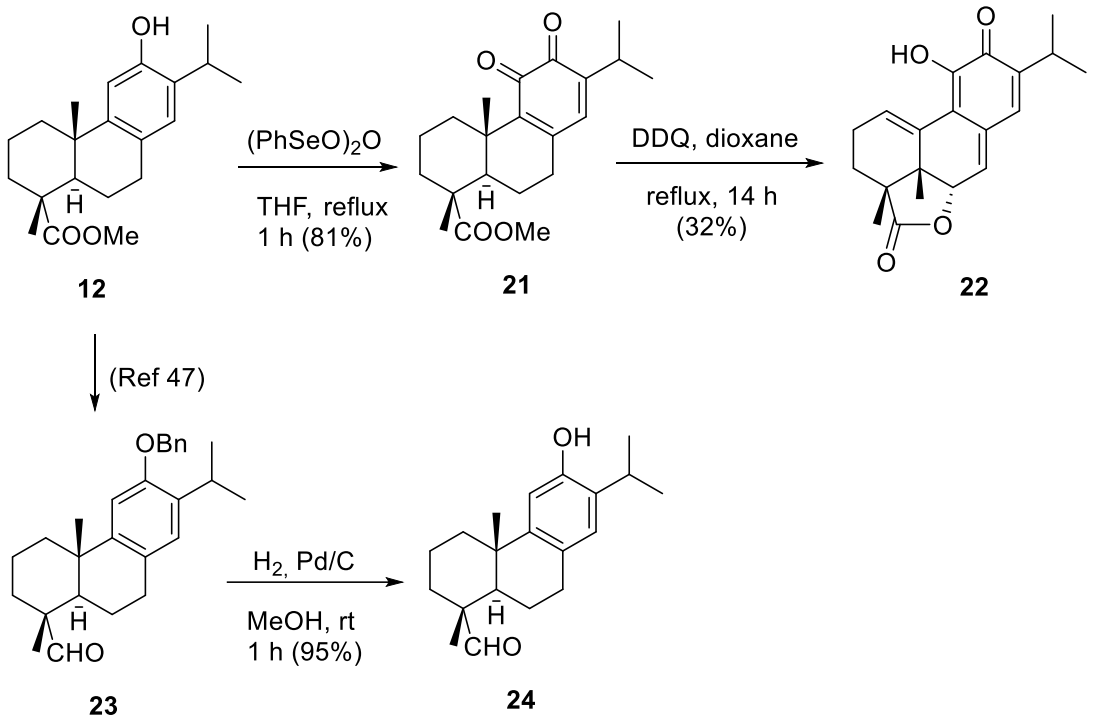

Scheme 3. Synthesis of Lactone **22** and 18-Oxoferruginol (**24**) from Hydroxy Ester **12**.

Finally, taxodal (**8**) and cupressol (**9**) were synthesized starting from 12-*O*-methylsugiol (**25**), a natural terpenoid,[49] also available from other natural abietane diterpenoids (Scheme 4).[50] The reduction of ketone **25**, and subsequent dehydration of the resulting alcohol gave alkene **26,**[51,52] which was transformed into the tetrahydrofluorene derivative **27**, utilizing a new patented procedure developed in our laboratory.[53] The reductive ozonolysis of the latter gave the new *O*-methyltaxodal (**28**), that was readily transformed into the target compound **8.**[34,54] The treatment of methylether **28** with $NaClO_2$ gave a 1:2.5 mixture of 12-*O*-methylcupressol **29**[49] and its 5-epimer **30**, that were subsequently being converted into the corresponding phenolic derivatives, cupressol (**9**)[35] and its epimer **31**, respectively.

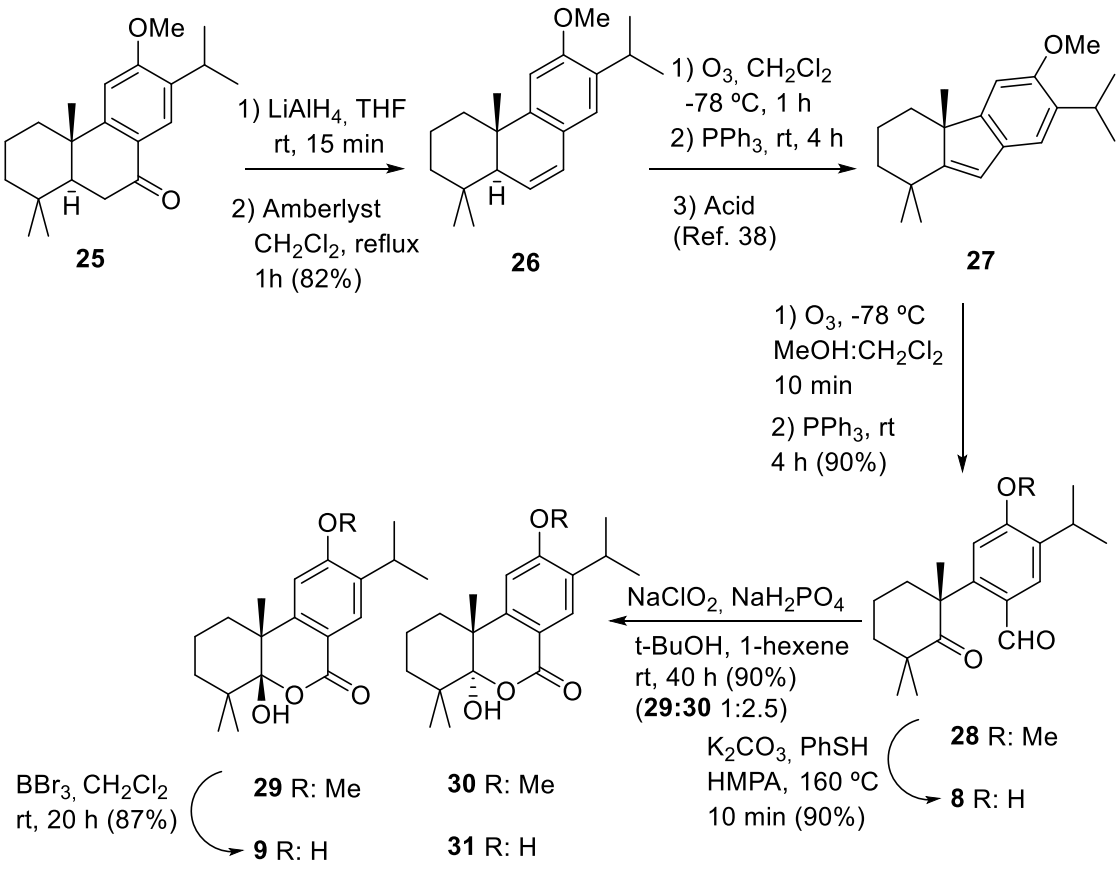

Scheme 4. Synthesis of Taxodal (**8**) and Cupressol (**9**) from 12-*O*-methylsugiol (**25**).

In Vitro Trypanocidal Activity. The oxidized abietane and nor-abietane terpenoids **8**, **9**, **14**, **15**, **20**, **22** and **24**, together with hanagokenol A and fortunin H, two natural synthetic terpenoids,[47] were evaluated against the three morphological forms of *T. cruzi*. The replicative extracellular epimastigotes were used as a primary screening because they are easy to handle, and the potential compounds were then evaluated against the developed forms in vertebrate hosts, trypomastigote, and amastigote forms.[55] These are the relevant forms from a clinical point of view since they are responsible for the acute and chronic phases of the disease. Moreover, considering the genetic diversity of *T. cruzi*, its variable drug resistance to current treatments,[55,56] and the CD target product profile (TPP) established by the Drugs for Neglected Diseases *initiative* (DND*i*),[57] three different strains – belonging to three discrete typing units (DTUs) (TcI,

TcV, and TcVI) from different tropism, host and location, and different genotype and phenotype[58] – were utilised for the in vitro screening. The mammalian Vero cell line was used as the host cell and to determine the cytotoxicity of the compounds.

The trypanocidal activity and cytotoxicity of the compounds, expressed as the inhibitory concentration 50 (IC_{50}), are shown in Table 1. BZN was also included in order to compare their activities with the reference drug for CD. Moreover, the selectivity indices (SI = IC_{50} Vero cells/IC_{50} parasite) (Table S1, Supporting Information) were calculated to establish the selectivity of the compounds on *T. cruzi*. According to the bibliography, potential anti-Chagas agents must meet certain cut-offs: I) $IC_{50} \leq 10$ μM, SI > 10[59]; II) $IC_{50} < 5$ μM, SI > 10[60]; III) SI > 50.[61] Therefore, compounds **8** and **15** were prioritised as potential compounds for their evaluation in clinical forms after primary screening in the epimastigote forms ($IC_{50} < 20$, SI > 15). Subsequently, these compounds showed better trypanocidal activity than BZN in amastigote and trypomastigote forms, and fulfilled the most stringent requirements mentioned above (IC50 < 10, SI > 40). Moreover, these compounds were active against the three *T. cruzi* strains (included BZN-resistant SN3 strain), devoid of drug resistance.

In summary, **8** and **15** were chosen for the subsequent in vivo evaluation (Scheme 5) and MoA studies due to their promising trypanocidal activity and low toxicity. These trials were performed using only the *T. cruzi* Arequipa strain in order to reduce the number of animal testing, as there were no significant differences for the other evaluated strains.

Table 1. Trypanocidal Activity of Benznidazole and Compounds on the Three Developmental Forms of *Trypanosoma cruzi* Strains, and Toxicity on Mammalian Vero Cells.

Compound	Activity IC_{50} (µM)[a] *T. cruzi* Arequipa strain			Activity IC_{50} (µM)[a] *T. cruzi* SN3 strain			Activity IC_{50} (µM)[a] *T. cruzi* Tulahuen strain			Toxicity IC_{50} (µM)[b] Vero cell
	Epim. forms	Am. forms	Trypom. forms	Epim. forms	Am. forms	Trypom. forms	Epim. forms	Ama. forms	Trypom. forms	
BZN	16.9 ± 1.8	8.3 ± 0.7	12.4 ± 1.1	36.2 ± 2.4	16.6 ± 1.4	36.1 ± 3.1	19.7 ± 1.7	10.0 ± 0.8	15.1 ± 1.3	80.4 ± 7.1
8	18.5 ± 1.2	9.2 ± 1.0	9.9 ± 0.8	12.5 ± 1.4	7.2 ± 0.9	8.7 ± 0.7	13.5 ± 1.1	8.8 ± 0.7	9.3 ± 0.9	623.9 ± 54.2
9	40.5 ± 3.3	nd	nd	91.2 ± 7.8	nd	nd	72.8 ± 6.1	nd	nd	480.1 ± 32.4
14	75.0 ± 6.8	nd	nd	102.7 ± 11.8	nd	nd	71.2 ± 6.2	nd	nd	101.8 ± 14.2
15	1.4 ± 0.3	4.8 ± 0.5	0.7 ± 0.1	1.6 ± 0.2	5.4 ± 0.4	1.8 ± 0.1	2.1 ± 0.2	7.1 ± 0.8	1.6 ± 0.2	72.2 ± 5.8
20	19.0 ± 1.2	nd	nd	13.5 ± 2.2	nd	nd	19.2 ± 2.3	nd	nd	26.1 ± 3.5
22	75.9 ± 6.7	nd	nd	110.1 ± 13.0	nd	nd	95.3 ± 9.9	nd	nd	222.4 ± 21.0
24	59.5 ± 4.3	nd	nd	63.0 ± 7.1	nd	nd	48.7 ± 3.9	nd	nd	106.5 ± 11.7
Hanagokenol A	51.0 ± 4.8	nd	nd	60.8 ± 7.1	nd	nd	62.8 ± 7.3	nd	nd	951.7 ± 73.8
Fortunin H	31.1 ± 2.4	nd	nd	36.7 ± 4.4	nd	nd	34.6 ± 5.0	nd	nd	762.8 ± 61.9

[a] Inhibition concentration 50 (IC_{50}), concentration (µM) required to inhibit 50% population, determined using GraphPad Prism 6. [b] Towards Vero cells. Values are the means of three separate determinations ± standard deviation. BZN, benznidazole. nd, not determined.

As can be deduced from the foregoing, the royleanone related quinones **15** and **20** are among the most active compounds. Changing the C-4-methoxycarbonyl by a methyl group, increases considerably the activity (compound **15** vs. compound **20**). Furthermore, the presence of the Δ^6 double bond in quinone **15** significantly increases the biological activity.[62] On the other hand, taxodal (**8**), with a *nor*-abietane skeleton and whose antifungal activity had previously been reported,[34] also exhibited a considerable activity.

Ultimately, the average number of amastigotes per Vero cell was also measured to acquire more accurate information regarding the most active terpenoids (Figure 2). The number of amastigotes per cell gradually decreased in all cases after a 72 h exposure, highlighting that the effect of the tested compounds at 50 μM reduced the number of amastigotes to practically 0. These data show that **8** and **15**, like BZN, could be considered as fast-acting trypanocidal drugs. The time to kill is another important feature to predict the exposure needed to avoid any relapse after in vivo chemotherapy, and it is questionable whether a slow-acting drug is desirable.[60]

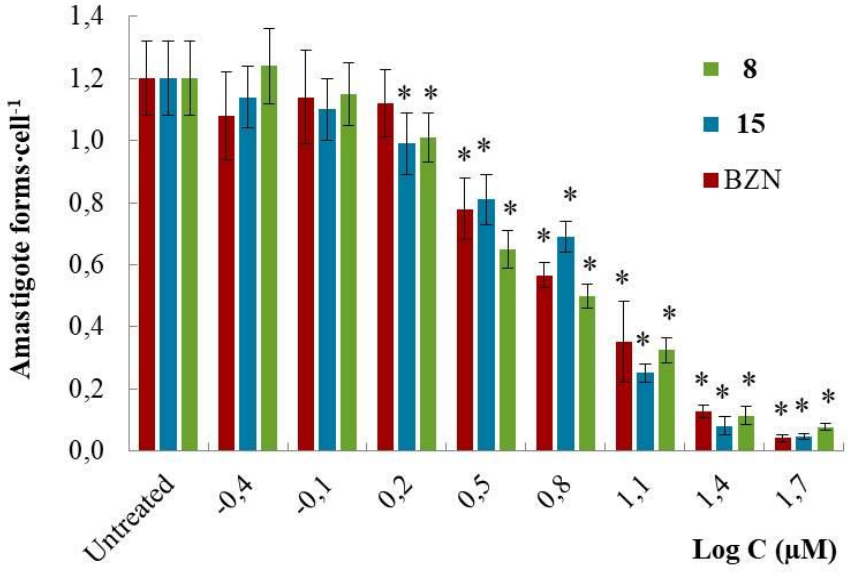

Figure 2. Number of amastigotes of *Trypanosoma cruzi* Arequipa strain per Vero cell exposed to benznidazole (BZN), **8** and **15**. Values constitute means of three separate determinations ± standard deviation. *Significant differences between untreated and treated parasites are tested at $\alpha = 0.05$.

In conclusion, terpenoids **8** and **15** met the majority of the in vitro criteria established by Chatelain including IC_{50} and SI (mentioned above), efficacy against a panel of different genotypes/strains, and the time to kill (fast-acting drug).[60]

In Vivo Trypanocidal Activity. Terpenoids **8** and **15** were selected for the in vivo evaluation in BALB/c mice based on the promising results in relation to their high in vitro trypanocidal activity against amastigote and trypomastigote forms, low toxicity, broad spectrum of action, and fast-acting behaviour. The in vivo evaluation was carried out in both the acute and chronic phases of the disease (Scheme 5) due to the different effectiveness of current treatments, which relatively have limited efficacy in the chronic CD.[24,63,64] The oral administration of the compounds was followed since it is the preferred therapeutic route for parasitic diseases in developing countries because of its low cost and its association with better patient compliance according to the TPP established by the DND*i*.[57,65] It should be noted that most in vivo testing has focused on the acute phase infections, partially because it is easier to monitor its parasite burden.[66–69] However, the ability to cure chronic phase infections is still a major need from a clinical viewpoint.[57] Therefore, the different phase-specific drug responses highlight the importance of studying the chronic phase infections in animal models.

The treatment guideline was at the subcurative doses of BZN (20 $mg \cdot kg^{-1}$ per day, 5 consecutive days) in order to evaluate whether the tested terpenoids would demonstrate a

higher in vivo trypanocidal activity than BZN. Moreover, it is defined that a compound showing a reasonable parasitaemia reduction in infected mice following 5 days of treatment can be considered a lead compound.[60]

The effectiveness of the tested terpenoids was assessed by determining the parasitaemia profile by counting bloodstream trypomastigotes during the acute phase, and the parasitaemia reactivation after immunosuppression (IS) and the nested parasites in organs by PCR in the chronic phase. In addition, the levels of immunoglobulin G (IgG) and the splenomegaly were measured as indicators of immune response, which are linked with the parasitic load.[70,71]

Figure 3 shows the parasitaemia profile of each group of mice during the acute CD until 55th dpi, when the parasitaemia was detected negative. All treated mice showed a significant reduction of parasitaemia, with a prominent effect of terpenoid **15**. Compound **15**-treated mice showed reduction of parasitaemia from the beginning of the treatment, with parasitaemia even disappearing on the 13th dpi. Furthermore, the performance of compound **15** was maintained like that of BZN until the 35th dpi. Additionally, compound **15** caused a reduction of around 65% in the parasitaemia peak compared to untreated mice, and it resolved the infection 7 days earlier than BZN and other groups. Significant differences were also observed 1 day after the treatment had finished between untreated and compound **2**-treated mice, but an increase in the parasitaemia levels were observed later, perhaps due to its rapid metabolism. A long-term treatment could be performed to achieve a better result due to its low toxicity as it will be discussed later in this section.

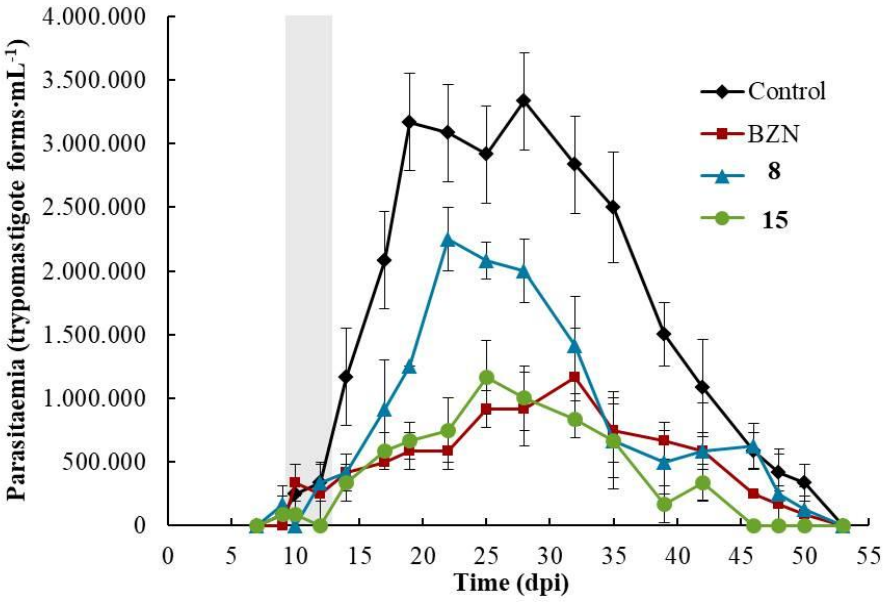

Figure 3. Parasitaemia profile of each group of mice infected with *Trypanosoma cruzi* and treated during the acute Chagas-Disease over a period of 55 days: control (untreated), benznidazole (BZN), **8** and **15**. Grey bar represents the treatment length. Values are the means of three mice data ± standard deviation. Significant differences between untreated and treated mice are tested at $\alpha = 0.05$.

The experimental cure in infected mice was evaluated using a double checking procedure that is based on the IS and PCR of the target organs/tissues.[58,72] These techniques were used to determine the survival rate of the parasites and the disease extent in the late chronic phase to evaluate the treatment effectiveness. First, the mice were injected with the immunosuppressant cyclophosphamide monohydrate (CP) to block the immunological system with the objective of reactivating the parasitaemia under its control[73] and counting bloodstream trypomastigotes. At the end of the experiment, the mice were sacrificed and necropsied to harvest the target organs/tissues in order to confirm the presence of nested parasites by PCR, a method that shows better sensitivity than other blood methodologies.[74]

Recently, new bioluminescence in vivo imaging models involving the use of transgenic *T. cruzi* parasites have made it possible to follow the course and the dynamic of an infection, reducing the number of animals needed,[75,76] and generating data with superior accuracy.[77] Nevertheless, this experiment was aimed at providing evidence of cure, or a considerable reduction in the parasitic load, substantiated by the double checking in three independent mice samples. Hence, the animals that did not show parasitaemia reactivation and did show negative PCR data after the IS were considered cured.[58,78]

Figure 4A shows the reactivation percentages of the infection for each group of mice in both the acute and chronic phases of CD, which are proportional to the parasite survival rates. BZN-treated mice in the chronic phase showed lower parasitaemia reactivation than those treated in the acute phase (68.3 and 81.5%, respectively). It is well-known that BZN shows sterile cure in *T. cruzi* infections in murine models more readily in the chronic phase than in the acute phase. This is probably because the parasite burden is significantly low and limited to far few locations[72] The in vivo trypanocidal activity of quinone 15 was remarkable. The parasitaemia reactivation in compound **15**-treated mice was lower (~52%) than that in BZN-treated mice in both treatment phases. In contrast, higher percentages of reactivation were observed in compound **8**-treated mice in both phases. The parasitaemia reactivation pattern was expected for the mice treated in the acute phase and consistent with the parasitaemia profile. Fortunately, this pattern was also shown in mice treated in the chronic phase, providing the desirable drug response in both phases of CD.

The PCR results for the target organs/tissues for each group of mice are shown in Figure 4B. The detection for the parasite was positive in seven of the nine organs/tissues

defined as target organs/tissues,[58] probably due to the spatiotemporal dynamic distribution of the parasite during chronic infections, with foci that appear and disappear over the course of even a single day.[76] As expected, BZN-treated mice showed a higher percentage of parasite-free organs/tissues after treatment in the chronic phase than that after the acute phase (42.9 and 28.5%, respectively). For taxodal (**8**), we observed the same percentages of parasite-free organs/tissues as BZN in both phases of treatment. The treatment with quinone **15** resulted in 57.1% of parasite-free organs/tissues in both the acute and chronic phases of CD. To summarize, compound **15** showed the best trypanocidal activity after the double checking of the cure, and it even surpassed BZN, confirming the partial curative effect at the dosage tested in both phases of CD.

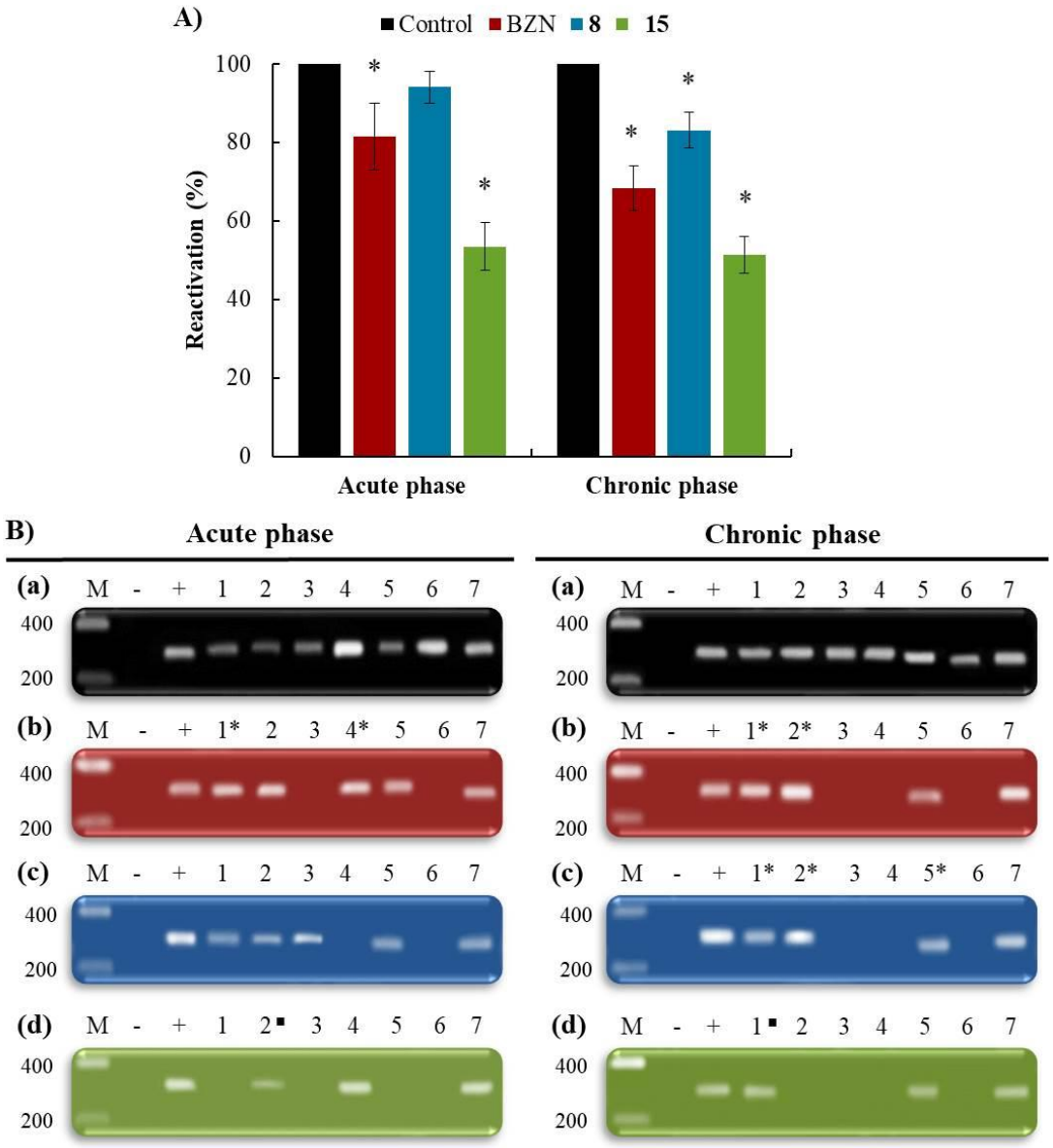

Figure 4. A) Parasitaemia reactivation by fresh blood after the IS cycles for each group of mice: control (untreated), benznidazole (BZN), **8** and **15**. Values are the means of three mice ± standard deviation. * Significant differences between untreated and treated mice at α = 0.05. **B)** PCR analysis of nine organs/tissues with the *Trypanosoma cruzi* Spliced Leader (SL) intergenic region sequence in chronic Chagas-Disease for each group of mice treated during the acute and chronic phases of the disease: (a) control (untreated), (b) benznidazole,

(c) **8** and (d) **15**. Lanes: (M) base pair marker, (-) PCR negative control, (+) PCR positive control, and (1-7) organs/tissues PCR: (1) adipose, (2) bone marrow, (3) brain, (4) oesophagus, (5) heart, (6) lung, and (7) muscle. ▪ 1/3 of the corresponding organ/tissue PCR products showed 300 bp band on electrophoresis; * 2/3 of the corresponding organ/tissue PCR products showed 300 bp band on electrophoresis.

The immune response of the mice was assessed by measuring the IgG levels and the splenomegaly as spleen is a main organ involved in defence against infections. These two measures were used to reveal the infection rates[58,71] and verify the effectiveness attributed to the treatment. Figure S1 (Supporting Information) shows the anti-*T. cruzi* IgG levels and the splenomegaly for each group of mice. All these data reflected the in vivo trypanocidal activities previously observed. Regarding the ELISA testing (Figure S1A, Supporting Information), it has to be mentioned that the samples obtained after the IS were used to confirm the IS suffered by the mice, but not to reflect the infection rates. Moreover, the 106th dpi samples were the only ones that did not show decreased levels of the parasites in all treated mice, presumably because they were samples from mice that had suffered an acute phase without treatment. Splenomegaly (Figure S1B, Supporting Information) is a major characteristic of chronic CD in mice and defined as the doubling of spleen mass compared to that from uninfected mice[58,70]. The treatment with quinone **15** not only reduced the parasite burden, but also greatly reversed the spleen enlargement, exhibiting spleen masses very close to those of uninfected mice.

On the other hand, the possible metabolic abnormalities associated with the treatment were determined by measuring kidney, heart, and liver biochemical markers (Table S2, Supporting Information), including values for uninfected mice. Although most

of the clinical parameters showed alterations 2 days post-treatment, they returned to normal levels as proved by the measurements obtained on the necropsy day. Terpenoids **8** and **15** showed even lower levels of disturbance on the necropsy day than the reference drug BZN. Moreover, it is noteworthy that none of the mice died nor lost more than 10% of body mass during and/or after treatment. The absence of toxicity allows these compounds to be studied at higher treatment doses to establish an improved treatment schedule based on pharmacokinetic studies in order to reach a sterile cure. It is well-known that adequate pharmacokinetics could achieve better in vivo results.[79]

Altogether, compound **15** fulfilled the majority of the in vivo criteria of the TPP, and according to the results, we suggest that it exhibits a satisfying ADMET profile.

MoA Analysis. The MoA analysis was performed at the energy metabolism level owing to the fast-acting trypanocidal activity showed by terpenoids **8** and **15** that can be explained by a bioenergetic collapse.

Catabolic Alteration. It is well-known that *T. cruzi* is unable to completely degrade glucose to CO_2 in aerobic environments, excreting into the medium incomplete oxidized acids like pyruvic acid, succinic acid, or EtOH, among others.[80,81] Accordingly, different excreted metabolic intermediates were measured using ^{1}H NMR spectra and compared with those found for the untreated parasites in order to evaluate the effect of terpenoids at IC_{25} concentrations (Figure 5**)**. Both terpenoids disturbed the excretions of glycerol and EtOH – end products of secondary catabolic pathways – and succinic acid metabolites, indicating alterations in the glucose catabolism. Nonsignificant alterations were observed in the other metabolites. These alterations can probably be a consequence of a mitochondrial dysfunction since the main glycolytic pathway end products, such as succinic acid, are

directed to the tricarboxylic acid cycle in the mitochondria for ATP synthesis,[82] while the secondary catabolic pathways are activated to compensate for the energetic deficit after mitochondrial alteration.[80] Moreover, it has been found that alterations in succinic acid may also be a consequence of mitochondrial redox stress produced by the inhibition of the mitochondrion-resident Fe-SOD enzyme.[83] Accordingly, mitochondrial dysfunction assays and SOD inhibition studies were performed.

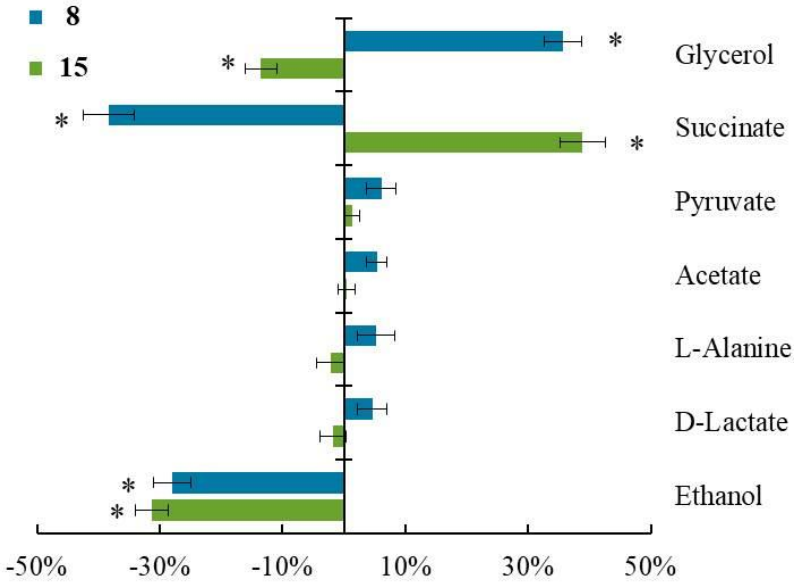

Figure 5. Variation among peaks of catabolites excreted by epimastigotes of *Trypanosoma cruzi* Arequipa strain exposed to terpenoids **8** and **15** at IC_{25} concentrations in comparison to control (untreated) parasites incubated 72 h. Values constitute means of three separate determinations ± standard deviation. * Significant differences between untreated and treated parasites at $\alpha = 0.05$.

Mitochondrial Dysfunction. In order to evaluate whether the activity of terpenoids **8** and **15** was a consequence of a dysfunction in the mitochondrial membrane potential, the parasites were exposed to terpenoids at IC_{25} concentrations. Figure 6 shows the flow

cytometry data, including KCN- and BZN-treated parasites. The results showed a membrane depolarization of 35.4% for BZN-treated parasites, which sounds logical since BZN kills *T. cruzi* through its metabolization into highly reactive species, such as glyoxal,[84] causing respiratory chain inhibition. Compared to BZN, the parasites treated with **8** and **15** showed a considerable membrane potential depolarisation, 41.8 and 50.0%, respectively. These dysfunctions can be attributed to the trypanocidal activity of terpenoids **8** and **15** that could produce a bioenergetic collapse, leading to *T. cruzi* death via necrosis in a mitochondrion-dependent manner. The proposed mechanism could also explain the fast-acting trypanocidal activity of these compounds.

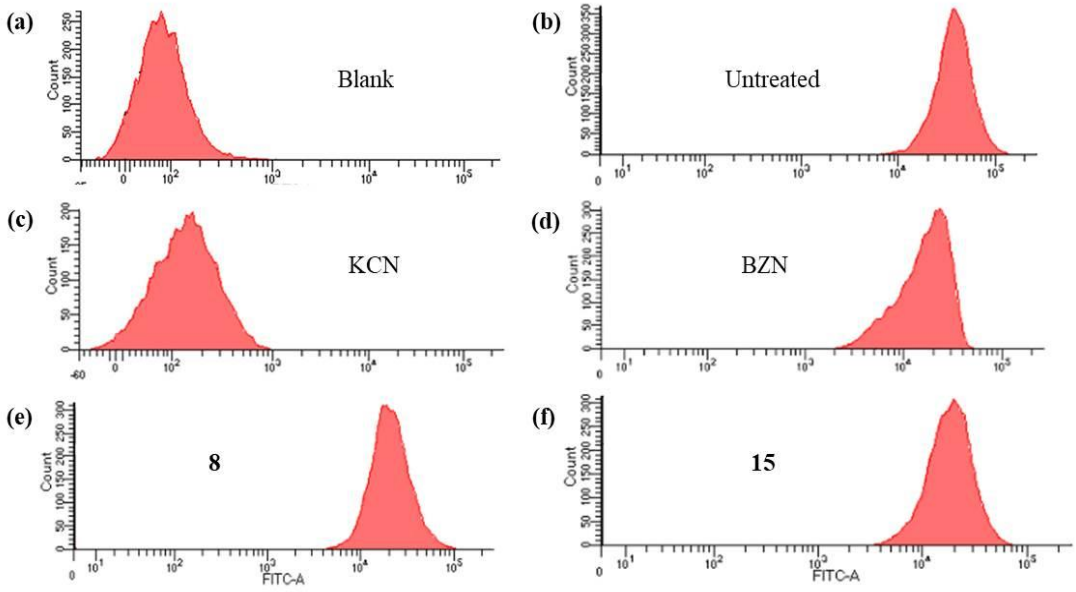

(g)

	Inhibition (%)		Inhibition (%)
KCN	95.5 ± 6.1	BZN	35.4 ± 3.2
8	41.8 ± 5.0	**15**	50.0 ± 5.5

Figure 6. Mitochondrial membrane potential for epimastigotes of *Trypanosoma cruzi* Arequipa strain exposed to different compounds at their IC_{25} concentrations incubated 72 h: (a) blank, (b) untreated (control), (c) KCN, (d) BZN, (e) **8**, and (f) **15**. (g) Inhibition, in

percentage, in mitochondrial membrane potential with respect to untreated parasites. Values constitute means of three separate determinations ± standard deviation. Significant differences between untreated and treated parasites at $\alpha = 0.05$.

The mitochondrion plays an imperative role in cell death decisions,[85] so disturbances in the membrane potential can cause an imbalance in the $NADH/NAD^+$ and ATP/ADP ratios, compromising the nucleic acid levels and causing necrosis and/or apoptosis.[80] Consequently, the nucleic acid levels were also measured by flow cytometry, as shown in Figure S1 (Supporting Information), together with the percentages of reduction in the nucleic acid levels. BZN-treated parasites suffered a 22.4% inhibition in nucleic acid levels. Whereas the parasites treated with terpenoids **8** and **15** showed a considerable inhibition (36.4 and 50.4%, respectively) in the nucleic acid levels. It must be noted that these inhibitions may not only result from ATP deficit, but also random nucleic acids degradation as a feature usually attributed to necrosis.[86]

SOD Inhibition. Since the trypanocidal activity of compounds **8** and **15** can be explained through a bioenergetic collapse caused by a mitochondrial dysfunction, mitochondrion-resident Fe-SOD inhibition studies were performed in order to evaluate whether the trypanocidal activity was ultimately due to the inhibition of this enzyme.[83] SOD is one of the most relevant therapeutic targets for CD treatment since it shows structural and biochemical differences with respect to the human CuZn-SOD, and it is a key enzyme in the protection against reactive oxygen species produced by oxidative stress.[87,88]

The SOD inhibition curves produced by compounds **8** and **15** are shown in Figure 7. As observed, neither compound **8** nor **15** had any inhibitory effect on human SOD. However, compound **15** caused a massive Fe-SOD inhibition with an IC_{50} value of 6.5 μM,

around 80% inhibition at 12.5 µM, and 100% inhibition at 25 µM. As a result, compound **15** could be suggested as a potent selective inhibitor of Fe-SOD. Although the trypanocidal effect of compound **15** can be ultimately ascribed to the inhibition of this enzyme, the possibility of multi-target activity should not be excluded.

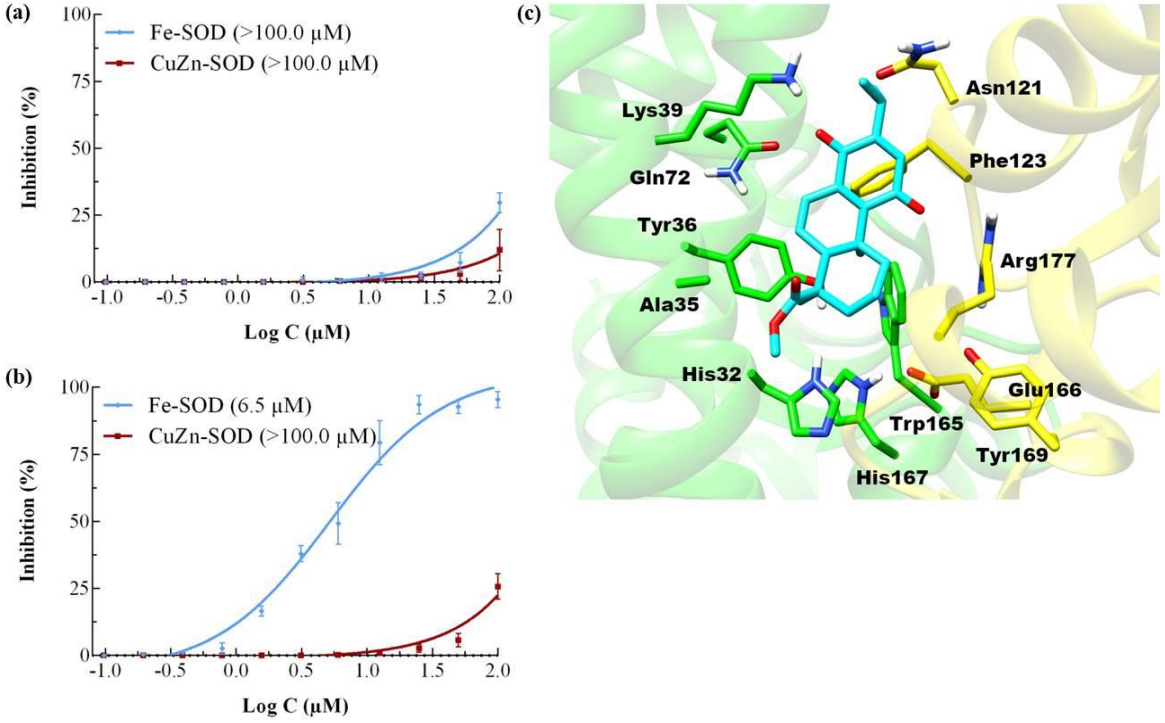

Figure 7. In vitro inhibition percentage of *Trypanosoma cruzi* Fe-SOD (activity 42.0 ± 3.8 U·mg^{-1}) and human erythrocytes CuZn-SOD (activity 47.3 ± 4.1 U·mg^{-1}) after treatment with (a) **8** and (b) **15**. Values constitute means of three separate determinations ± standard deviation. In brackets: IC_{50} value. (c) Proposed binding mode of compound **15** to the Fe-SOD enzyme (PDB ID 4DVH).[89] The compound is shown to bind in the dimer interface, and the interacting residues are shown as sticks. The following colour scheme was used: oxygen (red), nitrogen (blue), hydrogen (white), and carbon (protein chain A in yellow and

chain B in green, and compound **15** in cyan). Non-polar hydrogen atoms are not displayed. The figures were created by the software Chimera.

The binding mode of compound **15** to the Fe-SOD enzyme was explored by computational docking. In order to investigate the possible binding mode between compound **15** and its target, ligand-protein docking was performed following standard protocols.[90] The proposed binding mode is shown in Figure 7C. It has been reported that the aromatic groups of the drugs bind between residues of Phe123, Trp165, and Try36,[58,91] and this binding pattern was also observed for compound **15**. Moreover, the carbonyl groups on the quinone ring form hydrogen bonds with other important residues, namely Lys39 and Arg177.[58] While other groups in the molecule do not seem to be essential, and their binding changes from one series to the other.[58] In line with the previous observation, important interactions between the protein and the compound CH_3-C=O scaffold were not detected here. Even when possessing structural rigidity, compound **15** was able to fit into the binding cavity, allowing the aforementioned key interactions to occur. The rigidity of this molecule when compared to previous series could represent a gain in the total free energy that cannot be captured by docking by means of a decreased entropy loss upon binding. Stemming from the fact that the decrease in a compound flexibility is an approach for rational drug design, this rigid structural scaffold needs to be considered in further studies.

Overall, the in vitro and in vivo evaluation of the trypanocidal activity of the proposed compounds revealed that quinone **15** showed a higher activity, larger spectrum of action, and lower toxicity than BZN. This compound fulfilled the most stringent in vitro requirements for potential anti-Chagas agents and the in vivo criteria of the TPP, and

showed a promising in vivo ADMET profile. Furthermore, quinone **15** exhibited a higher trypanocidal activity than BZN in both the acute and chronic CD, as indicated by the different approaches, including parasitaemia monitoring, PCR, and IS. The MoA analysis suggested that the fast-acting trypanocidal activity is mitochondrion-dependent through a bioenergetic collapse caused by a mitochondrial membrane depolarisation and Fe-SOD inhibition. It is worth considering higher doses, different treatment schedules, and/or combined therapies in order to obtain a sterile cure. Collectively, quinone **15** can represent an affordable molecule with potential to be developed into a new anti-Chagas agent.

EXPERIMENTAL SECTION

CHEMISTRY

Experimental procedures, product characterizations, and ^{1}H and ^{13}C NMR spectra are included in the Supporting Information.

BIOLOGICAL ASSAYS

Animal and Parasitological Material. Epimastigote forms of three different *T. cruzi* strains – Arequipa strain of MHOM/Pe/2011/Arequipa (DTU) V),[58] SN3 strain of IRHOD/CO/2008/SN3 (DTU I),[92] and Tulahuen strain of TINF/CH/1956/Tulahuen (DTU VI),[58] – were cultured at 28 ºC in Gibco® RPMI 1640 Medium supplemented with 10% (v/v) heat-inactivated foetal bovine serum (FBS), 0.03M hemin and 0.5% (w/v) BBL trypticase.[93] Female BALB/c mice aged 10–12 weeks and weighed ~20 g were maintained under standard conditions of a 12 hour light/dark cycle with access to water and food ad libitum.

Screening Against Extracellular Epimastigotes. Trypanocidal activity against epimastigote forms was tested as previously described.[58] Briefly, parasites collected in the exponential growth phase were seeded in 96-well plates at 5×10^5 mL^{-1}, and treated by adding the tested compounds at a concentration range from 100 to 0.5 µM in 200 $mL \cdot well^{-1}$ at 28 ºC for 48 h. BZN and untreated growth controls were also included. Resazurin sodium salt (Sigma-Aldrich) was subsequently added to be incubated with the parasites for further 24 h. The trypanocidal effect was determined by absorbance measurements (Sunrise reader™, TECAN), and the activity was expressed as the inhibition concentration 50 (IC_{50}) using GraphPad Prism 6 software. Each compound concentration was tested in triplicate in four separate determinations.

Stock solutions of the compounds and BZN were dissolved using DMSO (Panreac, Barcelona, Spain) at high concentrations to assay them as nontoxic DMSO concentrations (<0.01% v/v) on parasite growth.

Cytotoxicity Test on Vero Cells. Mammalian Vero cells (EACC No. 84113001) were cultured at 37 ºC in 95% humidified air and 5% CO_2 atmosphere in Gibco® RPMI 1640 Medium supplemented with 10% (v/v) heat-inactivated FBS.[94]

Cytotoxicity tests against Vero cells were performed as described previously.[58] Briefly, Vero cells were seeded in 96-well plates at 1.25×10^4 mL^{-1}, and treated by adding the tested compounds at a concentration range from 1000 to 20 µM in 200 $mL \cdot well^{-1}$ at 37 ºC for 48 h. BZN and untreated growth controls were also included. Resazurin sodium salt was subsequently added to be incubated with the cells for further 24 h. The cell viability was determined following the same procedure used to assess the trypanocidal activity in the

epimastigote forms. Each compound concentration was tested in triplicate in four separate determinations.

Screening Against Intracellular Amastigotes and Infected Cells. The trypanocidal activity against amastigote forms was evaluated following the protocols previously reported.[95] Briefly, the culture-derived trypomastigotes were used to infect 1×10^4 Vero cells·well^{-1} in 24-well plates with rounded coverslips at a multiplicity of infection (MOI) ratio of 1:10 for 24 h. The non-phagocyted trypomastigotes were washed and treated by adding the tested compounds at a concentration range from 50 to 0.5 µM in 500 mL·well^{-1} at 37 ºC in 95% humidified air and 5% CO_2 atmosphere. BZN and untreated growth controls were also included. After 72 h of incubation, the trypanocidal effect was determined based on the number of amastigotes and infected cells in MeOH-fixed and Giemsa stained preparations by analysing 500 host cells randomly distributed in microscopic fields, and the activity was expressed as the IC_{50} using GraphPad Prism 6 software. Each compound concentration was tested in triplicate in four separate determinations.

Screening Against Bloodstream Trypomastigotes (BTs). BTs were obtained through a cardiac puncture of the infected BALB/c mice during the parasitaemia peak. The blood was collected in a 7:3 blood:anticoagulant (3.2% sodium citrate) ratio, and diluted in Gibco® RPMI 1640 Medium supplemented with 10% (v/v) heat-inactivated FBS.[58] The trypanocidal activity was tested according to the method previously described[95] using 96-well microtiter plates with 2×10^6 trypomastigotes·mL^{-1} treated by adding the tested compounds at a concentration range from 50 to 0.2 µM in 200 mL·well^{-1} and kept at 37 ºC in 95% humidified air and 5% CO_2 atmosphere for 24 h. BZN and untreated growth

controls were also included. Resazurin sodium salt was added to be incubated with the trypomastigotes for further 4 h. Similarly, the trypanocidal activity was assessed following the procedure used for the epimastigotes. Each compound concentration was tested in triplicate in four separate determinations.

Ethics Statement For In Vivo Assays On BALB/c Mice. All animal work (protocols and procedures, Scheme 6) was performed under RD53/2013 and approved by the Ethics Committee on Animal Experimentation (CEEA) of the University of Granada, Spain.

Mice Infection and Treatment. Infection was carried out by intraperitoneal inoculation of 5×10^5 BTs of *T. cruzi* Arequipa strain per mouse in 0.2 mL PBS.[58] The infection was confirmed on the 9th day post-infection (dpi) when BTs were visible in the bloodstream.

The mice were treated through the oral route (~200 µL) once daily for 5 consecutive days. The treatment of mice in the acute phase began when the infection was confirmed (9th dpi). While the treatment in the chronic phase was established on the 100th dpi.[95]

The mice were divided into five groups (n = 3 per group): 0, negative control group (uninfected and untreated mice); I, positive control group (infected and untreated mice); II, BZN group (mice infected and treated with BZN); III, **8** group (mice infected and treated with **8**); IV, **15** group (mice infected and treated with **15**). The tested compounds and BZN were prepared at 2 mg·mL^{-1} in an aqueous suspension vehicle containing 5% (v/v) DMSO and 0.5% (w/v) hydroxypropyl methylcellulose, as previously reported.[72] Therefore, doses of 20 mg·kg^{-1} per day were administered for 5 consecutive days, and the vehicle only was administered in the negative and positive control groups.

Monitoring of Parasitaemia During the Acute Phase Treatment. Parasitaemia levels were determined by counting BTs from peripheral blood drawn from the mandibular vein and diluted at a ratio of 1:100, as previously described.[58] The fresh blood microscopic examination was performed until the day when parasitaemia was not detected. The number of BTs was expressed as parasites·mL^{-1}.

IS Doses. On the 115th dpi, IS was performed by the intraperitoneal injection of three doses of 200 mg·kg^{-1} of ISOPAC® CP at 3–4 day intervals, as previously reported.[70] Mice were closely monitored for side effects or secondary infections due to IS. Within 7 days after the last CP injection, parasitaemia was determined to calculate the reactivation rate by counting BTs according the procedure described above.[58]

Mice Sacrifice, Blood Collection, and Organs/tissues Extraction. After CP-induced IS, the mice were euthanised after CO_2 anaesthesia by exsanguination via cardiac puncture, and the blood was collected. Mice were eventually necropsied to harvest the 9 target organs/tissues: adipose, bone marrow, brain, oesophagus, heart, lung, muscle, spleen, and stomach.[58] These organs/tissues were immediately perfused with pre-warmed PBS to avoid contamination with BTs,[96] and stored at -80 ºC until DNA extraction. In addition, spleens were weighed to assess inflammation (splenomegaly).[58]

Tissue DNA Extraction, PCR, and Electrophoresis. DNA extraction of the post-mortem organs/tissues was performed using Wizard® Genomic DNA Purification Kit,[97] and the extracted DNA was subjected to amplification by PCR based on the SL intergenic region sequence of *T. cruzi*. The amplification was performed using the commercial BioMix™ (Bioline) in a MyCycler™ Thermal Cycler (Bio-Rad). The PCR products were

resolved by electrophoresis on a 2% agarose gel (containing GelRed nucleic gel stain) for 90 min at 90 V.

ELISA Test. To obtain serum, blood samples were collected on several dpi (Scheme 6), and were processed according to the method previously described.[58] The serum samples were aliquoted to ELISA test and biochemical analysis. ELISA test was performed in 96-well plates using diluted serum samples 1:80 in PBS as previously described.[97] The excreted SOD from epimastigotes[58] was extracted, purified, and used as the antigen fraction. Blank and mouse negative control serum were also included. The absorbance measurements were read using a microplate reader (Sunrise reader™, TECAN).

Toxicity Test by Clinical Analysis. Aliquots of the serum samples (Scheme 5) were sent to the Biochemical Service of the University of Granada to measure a series of parameters with the commercial Cromatit® using a clinical chemistry analyzer (BS-200, Shenzhen Mindray Bio-medical Electronics Co., LTD). Mean and standard deviations were calculated using the levels measured for different populations of sera (n = 15, n = 3), and the confidence interval was calculated based on a confidence level of 95%.

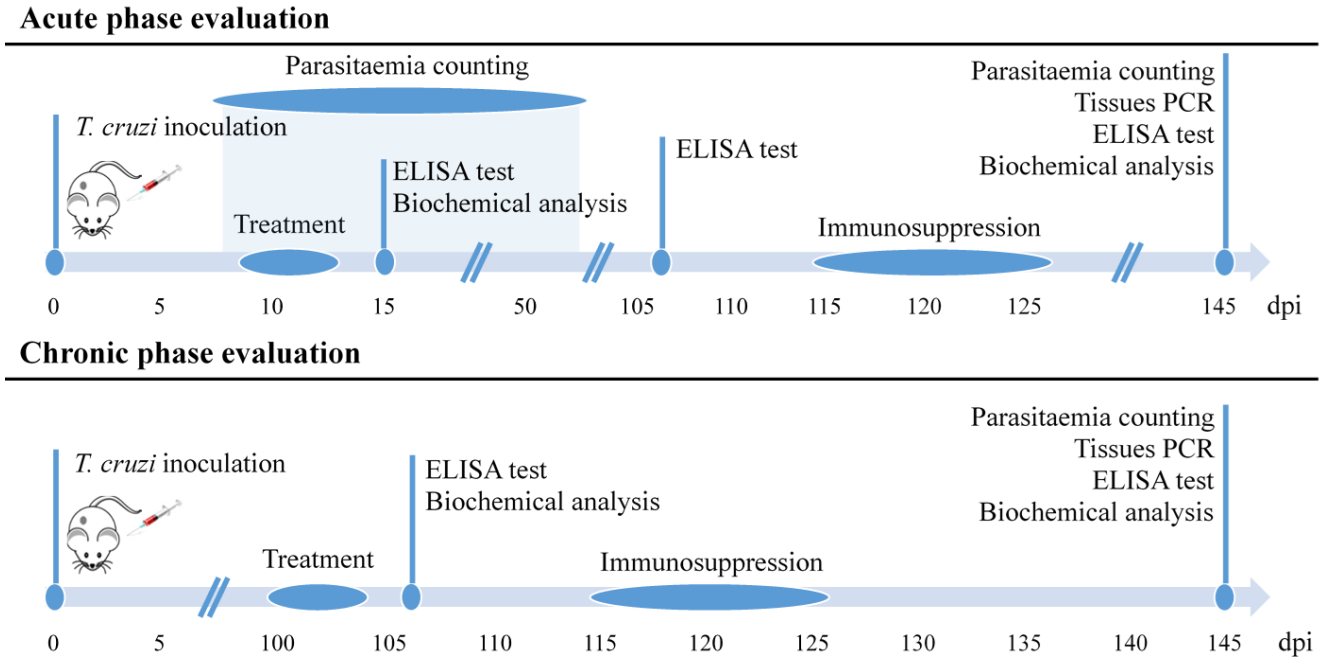

Scheme 5. Timeline for All in Vivo Assays on BALB/c Mice for the Evaluation of Compounds in the Acute and Chronic Phases of Chagas Disease. dpi = Day Post-Infection.

^{1}H NMR Analysis of Excreted Metabolites. Epimastigotes of *T. cruzi* Arequipa strain collected in the exponential growth phase were cultured in 25 cm^2 cell culture flasks at 5×10^5 ml^{-1}, and treated by adding the tested compounds at IC_{25} concentrations in 5 $mL \cdot flask^{-1}$ at 28 ºC for 72 h. Untreated controls were also included. The cultures were centrifuged and filtered to collect the supernatants for the ^{1}H NMR data analysis of the excreted metabolites using an NMR spectrometer (VARIAN DIRECT DRIVE 500 MHz Bruker) with AutoX probe, D_2O as a solvent, and 2,2-dimethyl-2-silapentane-5-sulphonate as the reference signal.[98] Chemical shifts were expressed in ppm, and the binning and normalisations were achieved using Mestrenova 9.0 software as well as the human metabolome database (http://www.hmdb.ca/). These characterizations were in agreement with the literature data.[98]

Flow Cytometry Analysis of Mitochondrial Membrane Potential and Nucleic Acid Levels. The epimastigotes of *T. cruzi* Arequipa strain described in the NMR analysis were collected by centrifugation, washed three times in PBS, and stained with 10 $mg \cdot mL^{-1}$ rhodamine 123 (Rho) (Sigma-Aldrich) or acridine orange (AO) (Sigma-Aldrich) dyes in 0.5 mL PBS for 20 min at 28 ºC.[99] Control epimastigotes with a fully depolarized mitochondrion were obtained by incubation for 40 min with 10 mM KCN prior to Rho loading.[100] Non-stained parasites were also included. After the incubation, the epimastigotes were immediately washed twice in ice-cold PBS and dispersed in 1 mL of cold PBS for the fluorescence analysis using a flow cytometer (BECTON DICKINSON FACSAria III) and a FACSDiva v8.01 software (BECTON DICKINSON).[58] The fluorescence intensities of Rho (FITC-A) and AO (APC-A) were quantified to determine the mitochondrial membrane potential and nucleic acids. The alterations in the fluorescence intensities were expressed as the index of variation (IV):

IV = (TM–CM)/CM, where TM and CM are the median fluorescence for treated and untreated epimastigote forms, respectively.[99]

SOD Enzymatic Inhibition Analysis. To obtain the Fe-SOD protein, epimastigotes of *T. cruzi* Arequipa strain collected in the exponential growth phase were cultured in 75 cm^2 cell culture flasks at 5×10^9 ml^{-1} in Gibco® RPMI 1640 Medium without FBS at 28 ºC for 28 h. The culture was subsequently centrifuged and filtered, and the supernatant was processed as previously described.[101] The protein content was quantified using the Bradford reagent (Sigma-Aldrich)[102] with bovine serum albumin (BSA) as a standard.

The in vitro activities of both the excreted Fe-SOD and commercial Cu/Zn-SOD from human erythrocytes (Sigma-Aldrich) were determined after exposing them to the tested compounds at a concentration range from 100 to 0.1 µM using the method previously described.[103]

Docking. The compounds were designed with the program Avogadro[104] after the estimation of their protonation state at pH 7.4 by the chemicalize web server (http://www.chemicalize.org/). The Chimera software[105] was used for calculating AM1 charges. The structure with Protein Data Bank (PDB) entry 4DVH was selected as a target for the docking, corresponding to the mitochondrial *T. cruzi* Fe-SOD protein.[89] The residue numbering of Martinez *et.al*, i.e., without the mitochondrial signal peptide, was used.[89] The protein protonation state at pH 7.4 was obtained by the program PDB2PQR.[106] The Autodock4.0 program was used for calculating Gasteiger charges[107] and performing the docking, with the Lamarckian genetic algorithm (LGA).[108] The docking was performed with a grid centered on the dimer interface.[90]

Statistical Analyses. Statistical analyses were performed by using SPSS software (v. 21, IBM). The t-test for paired samples was used to verify if there were

differences between the assays used ($p<0.05$, 95% confidence level). Statistical studies based on contingency tables (prevalence) were also conducted.

ASSOCIATED CONTENT

Supporting Information

Tables S1 and S2, figures S1 and S2, chemistry experimental procedures, product characterizations, and ^{1}H and ^{13}C NMR spectra of compounds.

AUTHOR INFORMATION

Corresponding Authors

Clotilde Marín – *Department of Parasitology, Instituto de Investigación Biosanitaria (ibs.Granada), Hospitales Universitarios De Granada/University of Granada, Severo Ochoa s/n, 18071 Granada, Spain;* https://orcid.org/0000-0002-4316-2742; Phone: +34 958 248 886; Email: cmaris@ugr.es

Enrique Álvarez-Manzaneda – *Departamento de Química Orgánica, Facultad de Ciencias, Instituto de Biotecnología, Universidad de Granada, 18071 Granada, Spain;* https://orcid.org/0000-0002-3659-4475; Phone: +34 958 248 089; Email: eamr@ugr.es

Authors

Rubén Martín-Escolano – *Department of Parasitology, Instituto de Investigación Biosanitaria (ibs.Granada), Hospitales Universitarios De Granada/University of Granada, Severo Ochoa s/n, 18071 Granada, Spain;* https://orcid.org/0000-0002-6262-9344

Juan J. Guardia – *Departamento de Química Orgánica, Facultad de Ciencias, Instituto de Biotecnología, Universidad de Granada, 18071 Granada, Spain.*

Javier Martín-Escolano – *Department of Parasitology, Instituto de Investigación Biosanitaria (ibs.Granada), Hospitales Universitarios De Granada/University of Granada, Severo Ochoa s/n, 18071 Granada, Spain.*

Nuria Cirauqui – *Molecular Microbiology and Structural Biochemistry, Université Claude Bernard Lyon 1, Centre National de la Recherche Scientifique, 69367 Lyon Cedex 07, France.*

Antonio Fernández – *Departamento de Química Orgánica, Facultad de Ciencias, Instituto de Biotecnología, Universidad de Granada, 18071 Granada, Spain.*

Maria J. Rosales – *Department of Parasitology, Instituto de Investigación Biosanitaria (ibs.Granada), Hospitales Universitarios De Granada/University of Granada, Severo Ochoa s/n, 18071 Granada, Spain.*

Rachid Chahboun – *Departamento de Química Orgánica, Facultad de Ciencias, Instituto de Biotecnología, Universidad de Granada, 18071 Granada, Spain.*

Manuel Sánchez-Moreno – *Department of Parasitology, Instituto de Investigación Biosanitaria (ibs.Granada), Hospitales Universitarios De Granada/University of Granada, Severo Ochoa s/n, 18071 Granada, Spain.*

Author Contribution

J.J.G., A.F., R.C. and E.A.-M. performed the synthesis and the chemical testing of the compounds.; R.M.-E. and J.M.-E. performed the in vitro and in vivo biological testing of the compounds; N.C. performed the computational docking; R.M.-E., M.J.R., M.S.-M, E.A.-M. and C.M. designed the experiments; R.M.-E., J.J.G., J.M.-E. and A.F. analysed the data; R.M.-E., J.J.G., N.C. and E.A.-M. wrote the manuscript; E.A.-M. and C.M. led the project team; The manuscript was written through contributions of all authors. All authors have given approval to the final version of the manuscript.

Notes

The authors declare no competing financial interest.

ACKNOWLEDGMENT

This research was supported by the Spanish Ministry of Economy and Competitiveness (CSD2010-00065 and CTQ2014-56611-R/BQU), including funds from the European Regional Development Fundings (ERDF). RM-E is grateful for the FPU Grant (FPU14/01537) from the Ministry of Education of Spain. We thank Ms. Amal S. Humidat for reviewing and correcting the English text.

REFERENCES

(1) Bern, C. N. *Engl. J. Med*. **2015**, *373*, 456–466.

(2) Hashimoto, K.; Yoshioka, K. *Adv. Parasitol.* **2012**, *79*, 375–428.

(3) Moncayo, Á.; Silveira, A. C. *Mem. Inst. Oswaldo Cruz.* **2009**, *104*, 17–30.

(4) DNDi - Drugs for Neglected Diseases initiative. https://www.dndi.org/diseases-projects/chagas/ (accessed March 20,2020).

(5) Hernández, C.; Vera, M. J.; Cucunubá, Z.; Flórez, C.; Cantillo, O.; Buitrago, L. S.; González, M. S.; Ardilla, S.; Zuleta Dueñas, L.; Tovar, R.; Forero, L. F.; Ramírez, J. D. *J. Infect. Dis. Adv*. **2016**, *214*, 1252–1255.

(6) Blanchet, D.; Frédérique, S.; Schijman, A. G.; Bisio, M.; Simon, S.; Véron, V.; Mayence, C.; Demar-pierre, M.; Djossou, F. *Infect. Genet. Evol*. **2014**, *28*, 245–250.

(7) Bastos, C. J. C.; Aras, R.; Mota, G.; Reis, F.; Dias, J. P.; De, R. S.; Prazeres, J.; Fernanda, M.; Grassi, R.; Freire, M. S.; de Araújo, E. G.; Prazeres, J.; Grassi, M. F. *PLoS Negl. Trop. Dis*. **2010**, *4*, 16–17.

(8) Pérez-Molina, J. A.; Norman, F.; López-Vélez, R. *Curr. Infect. Dis. Rep*. **2012**, *14*, 263–274.

(9) Bern, C.; Kjos, S.; Yabsley, M. J.; Montgomery, S. P. *Clin. Microbiol. Rev*. **2011**, *24*, 655–681.

(10) Requena-Méndez, A.; Aldasoro, E.; de Lazzari, E.; Sicuri, E.; Brown, M.; Moore, D. A.; Gascon, J.; Muñoz, J. *PLoS Negl. Trop. Dis*. **2015**, *9*, e0003540.

(11) Bern, C.; Montgomery, S. P. *Clin. Infect. Dis*. **2009**, *30341*, 52–54.

(12) Kessler, R. L.; Contreras, V. T.; Marliére, N. P.; Mazzarotto, A.; Batista, M.; Soccol, V. T.; Aurelio, *M. Mol. Microbiol.* **2017**, *104*, 712–736.

(13) Tyler, K. M.; Engman, D. M. *Int. J. Parasitol.* **2001**, *31*, 472–481.

(14) Tarleton, R. L. *Semin. Immunopathol*. **2015**, *37*, 233–238.

(15) Cardillo, F.; Teixeira Pinho, R.; Zuquim Antas, P. R.; Mengel, *J. Pathog. Dis.* **2015**, *73*, ftv082.

(16) Cunha-Neto, E.; Chevillard, C. *Mediators Inflamm*. **2014**, *2014*, 683230.

(17) Ribeiro, A. L.; Maria, P.; Teixeira, M. M.; Rocha, M. O. C. *Nat. Rev. Cardiol.* **2012**, *9*, 576–589.

(18) Pérez-molina, J. A.; Molina, I. *Lancet* **2018**, *391*, 82–94.

(19) Gaspar, L.; Moraes, C.; Freitas-Junior, L.; Ferrari, S.; Costantino, L.; Costi, M.; Coron, R.; Smith, T.; Siqueira-Neto, J.; McKerrow, J.; Cordeiro-da-Silva, A. *Curr. Med. Chem.* **2015**, *22*, 4293–4312.

(20) Molina, I.; Gómez i Prat, J.; Salvador, F.; Treviño, B.; Sulleiro, E.; Serre, N.; Pou, D.; Roure, S.; Cabezos, J.; Valerio, L.; Blanco-Grau, A.; Sánchez-Montalvá, A.; Vidal, X.; Pahissa, A. *N. Engl. J. Med*. **2014**, *370*, 1899–1908.

(21) Morillo, C. A.; Marin-Neto, J. A.; Avezum, A.; Sosa-Estani, S.; Rassi Jr, A.; Rosas, F.; Villena, E.; Quiroz, R.; Bonilla, R. Britto, C.; Guhl, F.; Velazquez, E.; Bonilla, L.; Meeks, B.; Rao-Melacini, P.; Pogue, J.; Mattos, A.; Lazdins, J.; Rassi, A.; Connolly, S. J.; Yusuf, S. *N. Engl. J. Med.* **2015**, *373*, 1295–1306.

(22) Morillo, C. A.; Waskin, H.; Sosa-Estani, S.; del Carmen Bangher, M.; Cuneo, C.; Milesi, R.; Mallagray, M.; Apt, W.; Beloscar, J.; Gascon, J.; Molina, I.; Echeverria, L. E.; Colombo, H.; Perez-Molina, J. A.; Wyss, F.; Meeks, B.; Bonilla, L. R.; Gao, P.; Wei, B.; McCarthy, M.; Yusuf, S. *J. Am. Coll. Cardiol*. **2017**, *69*, 939–947.

(23) Aldasoro, E.; Posada, E.; Requena-Méndez, A.; Calvo-Cano, A.; Serret, N.; Casellas, A.; Sanz, S.; Soy, D.; Pinazo, J.; Gascon, J. *J. Antimicrob. Chemother*. **2018**, *73*, 1060–1067.

(24) Wilkinson, S. R.; Taylor, M. C.; Horn, D.; Kelly, J. M.; Cheeseman, I. *Proc. Natl. Acad. Sci. USA* **2008**, *105*, 5022–5027.

(25) Mejia, A. M.; Hall, B. S.; Taylor, M. C.; Gómez-Palacio, A.; Wilkinson, S. R.; Triana-Chávez, O.; Kelly, J. M. *J. Infect. Dis*. **2012**, *206*, 220–228.

(26) Villarreal, D.; Barnabe, C.; Sereno, D.; Tibayrenc, M. *Exp. Parasitol.* **2004**, *108*, 24–31.

(27) Olmo, F.; Guardia, J. J.; Marin, C.; Messouri, I.; Rosales, M. J.; Urbanová, K.; Chayboun, I.; Chahboun, R.; Alvarez-Manzaneda, E. J.; Sánchez-Moreno, M. *Eur. J. Med. Chem*. **2015**, *89*, 863–890.

(28) Kusumoto, N.; Ashitani, T.; Hayasaka, Y.; Murayama, T.; Ogiyama, K.; Takahashi, K. J. *Chem. Ecol.* **2009**, *35*, 635–642.

(29) Ebrahini, S.; Zimmermann, S.; Zaugg, J.; Smiesko, M.; Brun, R.; Hamburguer, M. *Planta Med.* **2013**, *79*, 150–156.

(30) Matias, D.; Nicolai, M.; Saraiva, L.; Pinheiro, R.; Faustino, C.; Diaz Lanza, A.; Pinto Reis, C.; Stankovic, T.; Dinic, J.; Pesic, M.; Rijo, P. *ACS Omega* **2019**, *4*, 8094–8103.

(31) Tan, N.; Kaloga, M.; Radtke, O. A.; Kiderlen, A. F.; Öksüz, S.; Ulubelen, A.; Kolodziej, H. *Phytochemistry* **2002**, *61*, 881–884.

(32) Naman, C.; Gromovsky, A.; Vela, C.; Fletcher, J.; Gupta, G.; Varikuti, S.; Zhu, X.; Zywot, E.; Chai, H.; Werbovetz, K. A.; Satoskar, A. R.; Kinghorn, A. D. *J. Nat. Prod*. **2016**, *79*, 598–606.

(33) Burmistrova, O.; Simões, M.; Rijo, P.; Quintana, J.; Bermejo, J.; Estévez, F. *J. Nat. Prod.* **2013**, *76*, 1413–1423.

(34) Kusumoto, N.; Ashitani, T.; Murayama, T.; Ogiyama, K.; Takahashi, K. *J. Chem. Ecol*. **2010**, *36*, 1381–1386.

(35) Jolad, S.; Hoffmann, J.; Schram, K.; Cole, J.; Bates, R.; Tempesta, M. A. *J. Nat. Prod*. **1984**, *47*, 983–987.

(36) Alvarez-Manzaneda, E.; Chahboun, R.; Bentaleb, F.; Alvarez, E.; Escobar, M. A.; Sad-Diki, S.; Cano, M. J.; Messouri, I. *Tetrahedron* **2007**, *63*, 11204–11212.

(37) Bredenberg, J.; Gripenberg, *J. Acta Chem. Scand*. **1954**, *8*, 1728.

(38) Kang, J.; Li, L.; Wang, D.; Wang, H.; Liu, C.; Li, B.; Yan, Y.; Fang, L.; Du, G.; Chen, R. *Phytochemistry* **2015**, *116*, 337–348.

(39) Li, S.; Wang, P.; Deng, G.; Yuan, W.; Su, Z. *Bioorganic Med. Chem. Lett*. **2013**, *23*, 6682–6687.

(40) Choudhary, M.; Hussain, A.; Ali, Z.; Adhikari, A.; Sattar, S.; Ayatollahi, S.; Al-Majid, A. *Planta Med.* **2012**, *78*, 269–275.

(41) Ye, Y.; Wang, Y.; Yao, S.; Zhao, J.; Tang, C.; Xu, W.; Ke, C.; Xi, C. *PCT Int. Appl.* **2016**, WO 2016192631 A1 20161208.

(42) Chen, X.; Ding, J.; Ye, Y. M.; Zhang, J. S. *J. Nat. Prod.* **2002**, *65*, 1016–1020.

(43) Fujiwara, Y.; Mangetsu, M.; Yang, P.; Kofujita, H.; Suzuki, K.; Ohfune, Y.; Shinada, T. A. *Biol. Pharm. Bull.* **2008**, *31*, 722–725.

(44) Nagy, G.; Guènther, G.; Mathe, I.; Blundenc, G.; Yang, M.-H.; Crabb, T. *Phytochemistry* **1999**, *51*, 809–812.

(45) Miyajima, Y.; Saito, Y.; Takeya, M.; Goto, M.; Nakagawa-Goto, K. J. *Org. Chem.* **2019**, *84*, 3239–3248.

(46) Harrison, L. J.; Asakawa, Y. *Phytochemistry* **1987**, *26*, 1211–1212.

(47) Alvarez-Manzaneda, E.; Chahboun, R.; Alvarez, E.; Ramos, J.; Guardia, J. J.; Messouri, I.; Chayboun, I.; Mansour, A.; Dahdouh, A. *Synthesis* **2010**, *17*, 3493–3503.

(48) Ryu, Y. B.; Jeong, H. J.; Kim, J. H.; Kim, Y. M.; Park, J. Y.; Kim, D.; Naguyen, T. T. H.; Park, S. J.; Chang, J. S.; Park, K. H.; Rho, M. C.; Lee, W. S. *Bioorganic Med. Chem.* **2010**, *18*, 7940–7947.

(49) Wenkert, E.; Campello, J. de P.; McChesney, J. D.; Watts, D. J. *Phytochemistry* **1974**, *13*, 2545–2549.

(50) Thommen, C.; Jana, C.; Neuburger, M.; Gademann, K. *Org. Lett*. **2013**, *15*, 1390–1393.

(51) Su, W.; Fang, J.; Cheng, Y. *Phytochemistry* **1994**, *35*, 1279–1284.

(52) Gan, Y.; Li, A.; Pan, X.; Chan, A.; Yang, T.-K. *Tetrahedron* **2000**, *11*, 781–787.

(53) Alvarez-Manzaneda, E.; Chahboun, R.; Guardia, J. ES Patent 2547027 A1 20150930, **2015**.

(54) Kusumoto, N.; Murayama, T.; Kawai, Y.; Ashitani, T.; Ogiyama, K.; Takahashi, K. *Tetrahedron Lett*. **2008**, *49*, 4845–4847.

(55) Zingales, B. *Acta Trop*. **2017**, *184*, 38–52.

(56) Zingales, B.; Miles, M. A.; Moraes, C. B.; Luquetti, A.; Guhl, F.; Schijman, A. G.; Ribeiro, I. *Mem. Inst. Oswaldo Cruz.* **2014**, *109*, 828–833.

(57) DNDi Chagas disease target product profile. https://www.dndi.org/diseases-projects/chagas/chagas-target-product-profile/ (accessed March 22, 2020).

(58) Martín-Escolano, R.; Moreno-viguri, E.; Santivañez-Veliz, M.; Martín-Montes, Á.; Medina-Carmona, E.; Paucar, R.; Marín, C.; Azqueta, A.; Cirauqui, N.; Pey, A. L.;

Pérez-Silanes, S.; Sánchez-Moreno, M. J. *Med. Chem*. **2018**, *61*, 5643–5663.

(59) Don, R.; Ioset, J. R. *Parasitology* **2014**, *141*, 140–146.

(60) Chatelain, E. *J. Biomol. Screen*. **2014**, *20*, 22–35.

(61) Nwaka, S.; Besson, D.; Ramirez, B.; Maes, L.; Matheeussen, A.; Bickle, Q.; Mansour, N. R.; Yousif, F.; Townson, S.; Gokool, S.; Cho-Ngwa, F.; Samje, M.; Misra-Bhattacharya, S.; Murthy, P. K.; Fakorede, F.; Paris, J. M.; Yeates, C.; Ridley, R.; Van Voorhis, W. C.; Geary, T. *PLoS Negl. Trop. Dis.* **2011**, *5*, e1412.

(62) Ramírez-Macías, I.; Marín, C.; Es-Samti, H.; Fernández, A.; Guardia, J. J.; Zentar, H.; Agil, A.; Chahboun, R.; Alvarez-Manzaneda, E.; Sánchez-Moreno, M. *Parasitol. Int.* **2012**, *61*, 405–413.

(63) Scarim, C. B.; Jornada, D. H.; Chelucci, R. C.; De, L.; Leandro, J.; Chin, C. M. *Eur. J. Med. Chem*. **2018**, *155*, 824–838.

(64) Beaumier, C. M.; Gillespie, P. M.; Strych, U.; Hayward, T.; Hotez, P. J.; Elena, M. *Vaccine* **2016**, *34*, 2996–3000.

(65) Espuelas, S.; Plano, D.; Nguewa, P.; Font, M.; Palop, J. A.; Irache, J. M.; Sanmartín, C. *Curr. Med. Chem.* **2012**, *19*, 4259–4288.

(66) Chatelain, E.; Konar, N. *Drug Des. Devel. Ther*. **2015**, *9*, 4807–4823.

(67) Buckner, F. S. *Adv. Parasitol*. **2011**, *75*, 89–119.

(68) Canavaci, A. M. C.; Bustamante, J. M.; Padilla, A. M.; Brandan, C. M. P.; Laura, J.; Xu, D.; Boehlke, C. L.; Tarleton, R. L. *PloS Negl. Trop. Dis*. **2010**, *4*, e740.

(69) Romanha, A. J.; de Castro, S. L.; Correia Soeiro, M. N.; Lannes-Vieira, J.; Ribeiro, I.; Talvani, A.; Bourdin, B.; Blum, B.; Olivieri, B.; Zani, C.; Spadafora, C.; Chiari, E.; Chatelain, E.; Chaves, G.; Calzada, J. E.; Bustamante, J. M.; Freitas-Junior, L. H.; Romero, L. I.; Bahia, M. T.; Lotrowska, M.; Soares, M.; Gumes Andrade, S.; Armstrong, T.; Degrave, W.; Andrade, Z. *Mem. Inst. Oswaldo Cruz.* **2010**, *105*, 233–

238.

(70) Francisco, A. F.; Lewis, M. D.; Jayawardhana, S.; Taylor, M. C.; Chatelain, E.; Kelly, J. M. *Antimicrob. Agents Chemother*. **2015**, *59*, 4653–4661.

(71) Kayama, H.; Takeda, K. *Microbes Infect.* **2010**, *12*, 511–517.

(72) Francisco, A. F.; Jayawardhana, S.; Lewis, M. D.; White, K. L.; Shackleford, D. M.; Chen, G.; Saunders, J.; Osuna-Cabello, M.; Read, K. D.; Charman, S. A.; Chatelain, E.; Kelly, J. M. *Sci. Rep.* **2016**, *6*, 35351.

(73) Bustamante, J. M.; Craft, J. M.; Crowe, B. D.; Ketchie, S. A.; Tarleton, R. L. *J. Infect. Dis*. **2014**, *209*, 150–162.

(74) Martins, H. R.; Figueiredo, L. M.; Carneiro, C. M.; Bahia, M. T.; Pesquisas, D. *J. Antimicrob. Chemother*. **2008**, *61*, 1319–1327.

(75) Andriani, G.; Chessler, A. C.; Courtemanche, G.; Burleigh, B. A. *PLoS Negl. Trop. Dis*. **2011**, *5*, e1298.

(76) Lewis, M. D.; Fortes Francisco, A.; Taylor, M. C.; Burrell-Saward, H.; Mclatchie, A. P.; Miles, M. A.; Kelly, J. M. *Cell. Microbiol*. **2014**, *16*, 1285–1300.

(77) Lewis, M. D.; Francisco, A. F.; Taylor, M. C.; Kelly, J. M. J. *Biomol. Screen*. **2015**, *20*, 36–43.

(78) Santos, D. M.; Martins, T. A. F.; Caldas, I. S.; Diniz, L. F.; Machado-Coelho, G. L. L.; Carneiro, C. M.; Oliveira, R. de P.; Talvani, A.; Lana, M.; Bahia, M. T. *Acta Trop.* **2010**, *113*, 134–138.

(79) Urbina, J. A. *Curr. Pharm. Des*. **2002**, *8*, 287–295.

(80) Bringaud, F.; Rivière, L.; Coustou, V. *Mol. Biochem. Parasitol*. **2006**, *149*, 1–9.

(81) Maugeri, D. A.; Cannata, J. J. B.; Cazzulo, J. J. *Essays Biochem*. **2011**, *51*, 15–30.

(82) Wen, J.-J.; Gupta, S.; Guan, Z.; Dhiman, M.; Condon, D.; Lui, C.; Garg, N. J. J.

Am. Coll. Cardiol. **2010**, *55*, 2499–2508.

(83) Kirkinezos, I. G.; Moraes, C. T. *Semin. Cell Dev. Biol.* **2001**, 12, 449–457.

(84) Hall, B. S.; Wilkinson, S. R. *Antimicrob. Agents Chemother.* **2012**, *56*, 115–123.

(85) Lee, W.; Thévenod, F. *AJP Cell Physiol*. **2006**, *291*, C195-202.

(86) Verma, N. K.; Singh, G.; Dey, C. S. *Exp. Parasitol*. **2007**, *116*, 1–13.

(87) Maes, L.; Vanden Berghe, D.; Germonprez, N.; Quirijnen, L.; Cos, P.; De Kimpe, N.; Van Puyvelde, L. *Antimicrob. Agents Chemother*. **2004**, *48*, 130–136.

(88) Germonprez, N.; Maes, L.; Van Puyvelde, L.; Van Tri, M.; Tuan, D. A.; De Kimpe, N. *J. Med. Chem*. **2005**, *48*, 32–37.

(89) Martinez, A.; Peluffo, G.; Petruk, A. A.; Hugo, M.; Piñeyro, D.; Demicheli, V.; Moreno, D. M.; Lima, A.; Batthyány, C.; Durán, R.; Robello, C.; Martí, M. A.; Larrieux, N.; Buschiazzo, A.; Trujillo, M.; Radi, R.; Piacenza, L. *J. Biol. Chem*. **2014**, *289*, 12760–12778.

(90) Moreno-Viguri, E.; Jiménez-Montes, C.; Martín-Escolano, R.; Santivañez-Veliz, M.; Martin-Montes, A.; Azqueta, A.; Jimenez-Lopez, M.; Zamora Ledesma, S.; Cirauqui, N.; López De Ceráin, A.; Marín, C.; Sánchez-Moreno, M.; Pérez-Silanes, S. *J. Med. Chem*. **2016**, *59*, 10929–10945.

(91) Paucar, R.; Martín-Escolano, R.; Moreno-Viguri, E.; Azqueta, A.; Cirauqui, N.; Marín, C.; Sánchez-Moreno, M.; Pérez-Silanes, S. *Bioorg. Med. Chem*. **2019**, *27*, 3902–3917.

(92) Téllez-Meneses, J.; Mejía-Jaramillo, A. M.; Triana-Chávez, O. *Acta Trop*. **2008**, *108*, 26–34.

(93) Kendall, G.; Wilderspin, A. F.; Ashall, F.; Miles, M. A.; Kelly, J. M. *EMBO J.* **1990**, *9*, 2751–2758.

(94) Pless-Petig, G.; Metzenmacher, M.; Türk, T. R.; Rauen, U. *BMC Biotechnol.*

2012, *12*, 73.

(95) Martín-Escolano, R.; Molina-Carreño, D.; Delgado-Pinar, E.; Martín-Montes, A.; Clares, M. P.; Medina-Carmona, E.; Pitarch-jarque, J.; Martín-Escolano, J.; Rosales, M. J.; García-España, E.; Sánchez-Moreno, M.; Marín, C. *Eur. J. Med. Chem*. **2019**, 1*64*, 27–46.

(96) Ye, X.; Ding, J.; Zhou, X.; Chen, G.; Liu, S. F. *J. Exp. Med*. **2008**, *205*, 1303–1315.

(97) Olmo, F.; Rotger, C.; Ramírez-Macías, I.; Martínez, L.; Marín, C.; Carreras, L.; Urbanová, K.; Vega, M.; Chaves-Lemaur, G.; Sampedro, A.; Rosales, M. J.; Sánchez-Moreno, M.; Costa, A. *J. Med. Chem*. **2014**, *57*, 987–999.

(98) Fernández-Becerra, C.; Sanchez-Moreno, M.; Osuna, A.; Opperdoes, F. R. *J. Eukaryot. Microbiol*. **1997**, *44*, 523–529.

(99) Sandes, J. M.; Fontes, A.; Regis-da-Silva, C. G.; Brelaz De Castro, M. C. A.; Lima-Junior, C. G.; Silva, F. P. L.; Vasconcellos, M. L. A. A.; Figueiredo, R. C. B. Q. *PLoS One* **2014**, *9*, e93936.

(100) Abengózar, M. Á.; Cebrián, R.; Saugar, J. M.; Gárate, T.; Valdivia, E.; Martínez-Bueno, M.; Maqueda, M.; Rivas, L. *Antimicrob. Agents Chemother.* **2017**, *61*, e02288-16.

(101) López-Céspedes, Á.; Villagrán, E.; Briceño Álvarez, K.; de Diego, J. A.; Hernández-Montiel, H. L.; Saldaña, C.; Sánchez-Moreno, M.; Marín, C. *Sci. World J.* **2011**, *2012*, 914129.

(102) Bradford, M. *M. Anal. Biochem*. **1976**, *72*, 248–254.

(103) Beyer, W. F.; Fridovich, I. *Anal. Biochem*. **1987**, *161*, 559–566.

(104) Hanwell, M. D.; Curtis, D. E.; Lonie, D. C.; Vandermeersch, T.; Zurek, E.; Hutchison, G. R. J. *Cheminform*. **2012**, *4*, 17.

(105) Pettersen, E. F.; Goddard, T. D.; Huang, C. C.; Couch, G. S.; Greenblatt, D. M.; Meng, E. C.; Ferrin, T. E. *J. Comput. Chem*. **2004**, *25*, 1605–1612.

(106) Dolinsky, T. J.; Czodrowski, P.; Li, H.; Nielsen, J. E.; Jensen, J. H.; Klebe, G.; Baker, N. A. *Nucleic Acids Res*. **2007**, *35*, 522–525.

(107) Morris, G. M.; Huey, R.; Lindstrom, W.; Sanner, M. F.; Belew, R. K.; Goodsell, D. S.; Olson, A. J. *J. Comput. Chem*. **2010**, *30*, 2785–2791.

(108) Huey, R.; Morris, G. M.; Olson, A. J.; Goodsell, D. S. *J. Comput. Chem*. **2007**, *28*, 1145–1152.